

**Scientific and Technological Alliance for  
Guaranteeing the European Excellence in  
Concentrating Solar Thermal Energy**



FP7 Grant Agreement number: 609837  
 Start date of project: 01/02/2014  
 Duration of project: 48 months

***Project Deliverable 6.4:***

**Report on STE co-generation systems  
in agro-industrial applications**

<b>WP6 – Task 6.3</b>	<b>Deliverable 6.4</b>
<b>Due date:</b>	<b>October/2017</b>
<b>Submitted</b>	<b>January/2018</b>
<b>Partner responsible</b>	<b>LNEG</b>
<b>Person responsible</b>	<b>João Farinha Mendes</b>
<b>Author(s):</b>	<b>João P. Cardoso, Gilles Maag, Pedro H. S. Bezerra, Celso E. L. Oliveira, João Farinha Mendes</b>
<b>Document version:</b>	<b>1</b>
<b>Reviewed/supervised by:</b>	
<b>Dissemination Level</b>	<b>PU</b>

# Table of contents

---

1. Introduction .....	5
2. The agro-industrial sector in Brasil .....	7
2.1. Meat processing .....	8
2.2. Dairy plants .....	8
2.3. Sugar and ethanol mills .....	9
2.4. Integration of STE in agro-industrial applications .....	10
2.5. The SMILE project and the Pirassununga demonstration plant .....	11
3. Simulation of central tower receiver systems used in co-generation applications .....	13
3.1. Tools for simulation of central tower receiver systems .....	14
3.2. Plant model .....	15
3.2.1. Solar Field .....	15
3.2.2. Receiver model .....	17
3.2.3. Power block model .....	17
3.2.4. System model .....	19
3.2.5. Simulation of the Pirassununga facility .....	21
4. Scaling up to industrial plants .....	24
5. Bibliography .....	26

# Figures

---

Figure 1: Share in total energy consumption, 2011-12 (Organisation for Economic Co-operation and Development 2017). .....	6
Figure 2: Agrobusiness share of Brazilian GDP and its subdivision into stock farming and agriculture in 2014 (Instituto Brasileiro de Geografia e Estatística 2017). .....	7
Figure 3: Export products of the Brazilian agro-industrial sector in 2014. Source: GV Agro. ...	8
Figure 4: Trimestral raw milk production 2011-2016 (Instituto Brasileiro de Geografia e Estatística 2017). .....	9
Figure 5: Process schematic of the Pirassununga plant. ....	11
Figure 6: Process schematic of the Pirassununga Setup 1 plant. ....	12
Figure 7: Artist’s view of solar/biofuel hybrid plants of the SMILE project in Pirassununga (Setup 2, left) and Caiçara do Rio do Vento (right), Brazil. ....	12
Figure 8: Prototype of the 9 m <sup>2</sup> heliostat being employed in the SMILE project pilot plants. .	13
Figure 9: Installation site for Pirassununga solar plant in January 2018. ....	13
Figure 10: Optical efficiency matrices for Pirassununga Setup 1 (left), Pirassununga Setup 2 (center), and Caiçara (right). ....	16
Figure 11: Simplified layout for a gas turbine power block. ....	17
Figure 12: ORC power block. ....	19
Figure 13: TRNSYS model for the Pirassununga Setup 1 plant. ....	19
Figure 14: TRNSYS model for the Pirassununga Setup 2 plant. ....	20
Figure 15: Simulated operation temperatures for the STE system under construction in Pirassununga for a Summer day (1 <sup>st</sup> of February 2016). ....	23
Figure 16: Simulated operation temperatures for the STE system under construction in Pirassununga for a Spring day (11 <sup>th</sup> of May 2016). ....	24

# Tables

---

Table 1: Typical temperatures of main processes in the meat processing sector.....	8
Table 2: Type and amount of energy required for dairy goods production (Maganha 2006). ...	9
Table 3: Typical temperatures of main processes in the dairy sector.....	9
Table 4: Energy balance of typical sugar cane mill. ....	10
Table 5: Heliostat and simulation parameters for the Pirassununga plant, used for the determination of the optical efficiency matrices with Tonatiuh. ....	15
Table 6: Design point for the Pirassununga Setup 1 and 2 plants.....	20
Table 7: Comparison of the simulation results with the design values for the nominal operating point. ....	20
Table 8: Energy consumption of the Pirassununga USP campus abattoir.....	21
Table 9: monthly and annual energy flows in the Pirassununga Setup 2 plant. ....	22
Table 10: Energy consumption and operation schedule of typical Brazilian abattoirs. ....	25

## 1. Introduction

This report was produced within the scope of Work Package 6 (International Cooperation Activities), task 6.3 (Cooperation with Latin American Region), subtask 6.3.2 (Brazil), corresponding to project deliverable number 6.4.

One of the main objectives of WP 6 is to promote and enable cooperation between partners in Europe and different regions outside Europe with relevance to Solar Thermal Electricity (STE, also known as Concentrating Solar Power). This objective is pursued by the work developed in task 6.3.2 where Brazilian and Portuguese research institutions (USP and LNEG) are collaborating in central receiver systems research for the development of hybrid systems and cogeneration applications in the agro-industrial applications.

The scope of activities encompassed by the agro-industrial sector is not fully settled, with different definitions available and under discussion at international fora - mostly for statistical classification purposes (Ramaschiello 2015). For the purposes of this work agro-industry will be considered to be the subset of the manufacturing sector responsible for the processing of raw materials and intermediate products derived from agriculture, fisheries and forestry (Silva, et al. 2009). Under this definition, and considering the International Standard Industrial Classification, the agro-industrial sector encompasses: the food and beverages industry; tobacco industry; paper and wood industry; textiles, footwear and apparel industry; leather industry; natural rubber industry.

The agro-industrial sector is particularly relevant in developing countries where they account for a substantial share of industrial output – in African countries it can represent up to 50% of total manufacturing. This is especially true in the least-developed countries where the sector in conjunction with agriculture contribute between 20 to 30% of the Gross Domestic Product (United Nations 2017). Moreover, the sector is considered to be a strong driver for long term economic growth in developing countries.

This work will focus on the usage of Solar Thermal Electricity (STE) plants in the food and beverages industry, since this agro-industry sector has a strong presence in both industrialized and developing countries. It should be noticed however, that despite the significant presence in both kind of countries, its contribution towards the total value added of the manufacturing industry is very different, being well below 20% in industrialized countries and higher in developing countries (United Nations 2017).

The food processing industry is a significant energy consumer, representing on average approximately 2% of total energy consumption in both OECD and non-OECD countries, between 2011 and 2013. However, the total energy consumption of the sector significantly changes among countries, as visible in Figure 1. For the Brazilian case the food processing industry energy consumption is estimated to represent 10% of the total energy consumption. This value is lower for the EU28 where the food and beverage sector accounts for approximately 4% of the total energy consumption, corresponding to 10% of the energy consumed by the industrial sector (Organisation for Economic Co-operation and Development 2017). This energy demand is currently satisfied predominantly by fossil fuels.

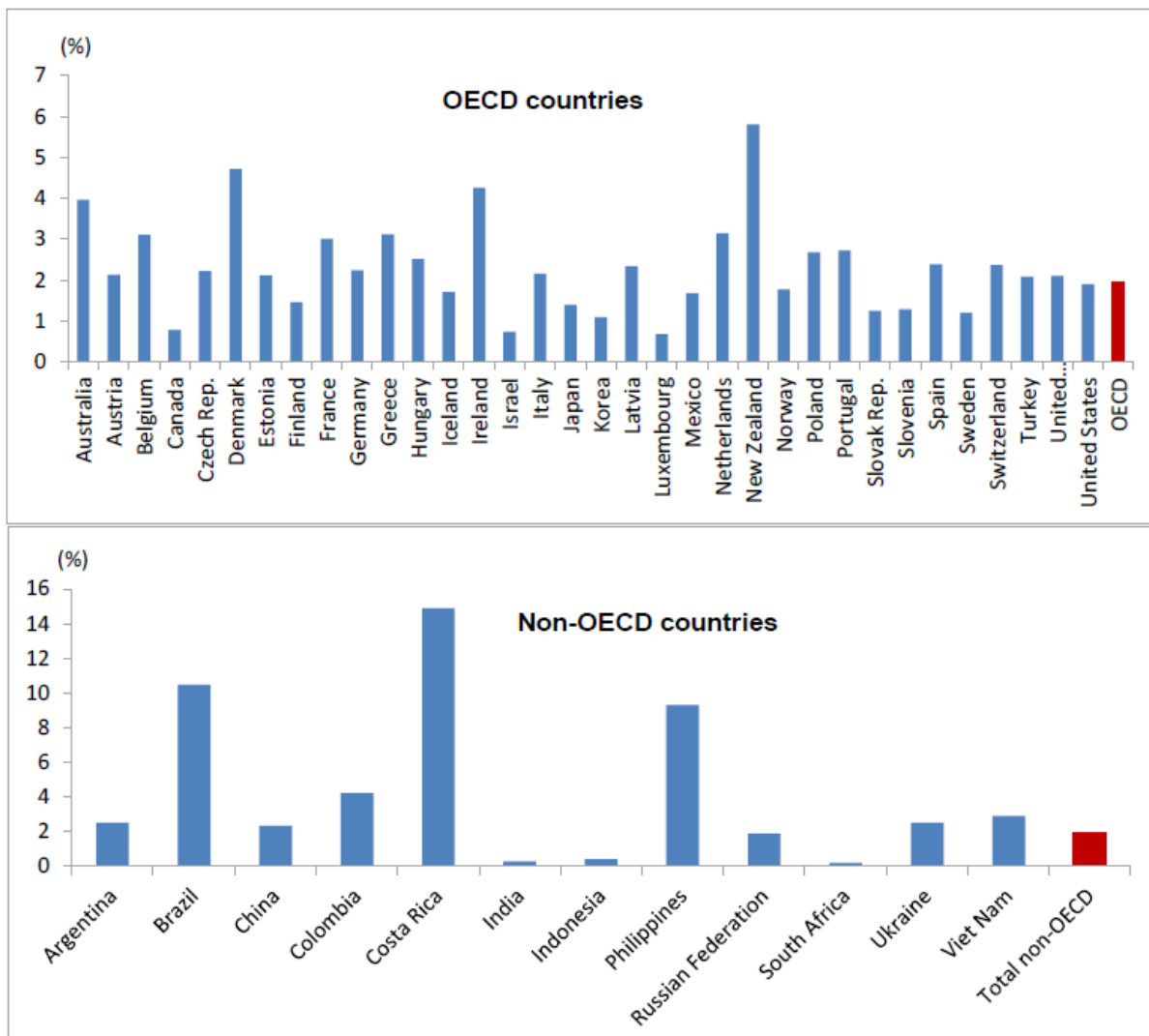


Figure 1: Share in total energy consumption, 2011-12 (Organisation for Economic Co-operation and Development 2017).

Considering the economic relevance of the agro-industrial sector and its significant energy demand, particularly noticeable in the food and beverage industry, it is imperative to promote energy efficiency measures and the introduction of renewable energy sources in order to reduce its environmental footprint, while promoting the sustainable development of both agro-industry and country. CSP plants can provide electricity and heat separately in dedicated plants or in co-generation, being suited to be integrated into agro-industrial processes. Additionally, they can be hybridized with biofuels, ensuring a continuous carbon free supply of energy to these industries.

This work focuses on the integration of energy produced by STE plants in the Brazilian agro-industrial sector. The Brazilian agro-industrial sector is briefly presented and the most suitable processes for the integration of electricity and heat co-generated by STE plants are identified and their energy needs are described. Two pilot facilities being built in Brazil are presented and simulations are performed to illustrate the operation of one of those pilot facilities. Additionally the feasibility of the integration of STE plants in the meat processing industry is studied.

## 2. The agro-industrial sector in Brasil

The Brazilian agro-industrial sector represents 21.3% of the country's Gross Domestic Product (GDP, Figure 2), corresponding to approximately 1.2 trillion R\$ (Reais: 1 € = 3.9 R\$ on December 1st 2017), according to the Brazilian Institute of Geography and Statistics IBGE. Together with the industrial sector it accounts for 40.3% (220 TWh) of Brazil's electricity and 35.5% of the total primary energy consumption (Ministério de Minas e Energia 2014). Due to the nature of the business, a significant part of agro-industrial energy consumers are located in places distant from urban centers – or even without access to the National Interconnected Grid (SIN – Sistema Interligado Nacional) – though usually with a good availability of space and often with annual DNI levels above 2000 kWh/m<sup>2</sup>, making them promising candidates for coupling with CSP/STE technologies for heat and power supply.

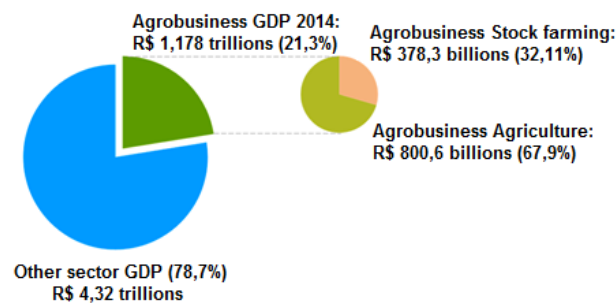


Figure 2: Agrobusiness share of Brazilian GDP and its subdivision into stock farming and agriculture in 2014 (Instituto Brasileiro de Geografia e Estatística 2017).

Brazilian agro-industrial products possess a high level of international market insertion and therefore exert a significant impact on the country's foreign income (Perobelli, et al. 2017). Between 2000 and 2013, the export revenue for agro-industrial goods grew by 230%, reaching approximately 100 billion euros by the end of said period (Perobelli, et al. 2017). In 2014, 61.2% of this revenue originated from three product groups: soy, meat, and sugar/ethanol (Instituto Brasileiro de Geografia e Estatística 2017). A graphic overview is shown in Fig. 2.

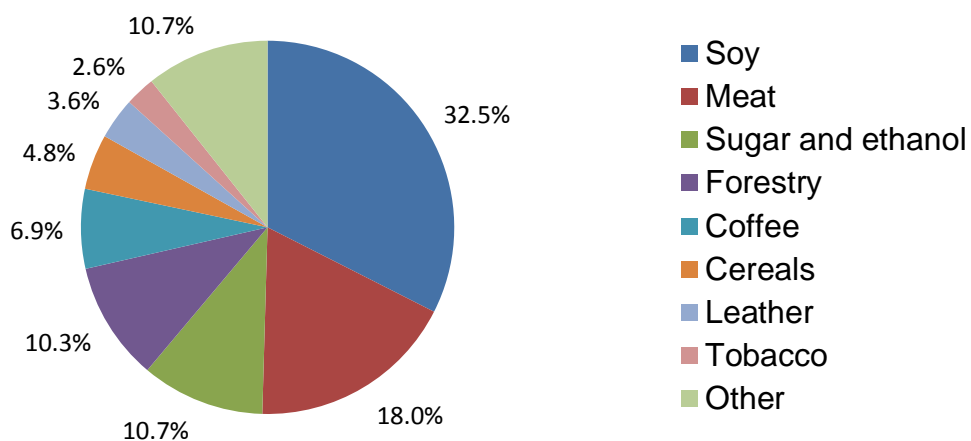


Figure 3: Export products of the Brazilian agro-industrial sector in 2014. Source: GV Agro.

Most of these processes require a supply of both electricity and heat, the latter usually delivered by boilers fuelled by biomass or fossil fuels. The identification of possible interactions between agro-industrial activities and solar thermal systems is a complex endeavour, being a function of the varying requirements between sectors, as well as between different technological solutions in the same sector (Hassine, et al. 2015).

Based on their energy consumption characteristics, the value added to the processed good, seasonal production volume patterns, and the international market to be served, the meat processing, dairy, and sugar cane sectors have been individuated as high-potential application fields for CSP/STE technologies.

## 2.1. Meat processing

In 2016, 30.6 million heads of cattle were processed in Brazil (Instituto Brasileiro de Geografia e Estatística 2017), with a projected yearly increase of 2.4% until 2026 (Ministério da Agricultura, Pecuária e Abastecimento 2016). Large-scale abattoirs and meat processing plants operate at daily capacities of 500-700 heads, on a 24/7 basis.

Total energy consumption per head of cattle in São Paulo state abattoirs strongly depends on their degree of automation and modernity. Values starting from 70 up to as much as 300 kWh per head are reported (Pacheco e Yamanaka 2006), of which 80-85% are heat, in form of hot water and water vapour up to 120 °C, for instance for sterilization and cleaning of process equipment and facilities. The remaining 15-20% are electricity consumption, ca. 60% of which are attributed to cooling (Pacheco e Yamanaka 2006).

Table 1 shows the main heat-consuming processes and their typical temperatures in the meat processing sector.

<b>Process</b>	<b>Medium</b>	<b><math>T</math> (°C)</b>
Ambient and equipment sterilization and cleaning	Water/vapor	60-120
Cooking	Water	90-100

Table 1: Typical temperatures of main processes in the meat processing sector.

## 2.2. Dairy plants

Yearly national raw milk production was 34.2 billion litres in 2016 (Instituto Brasileiro de Geografia e Estatística 2017). Figure 4 shows raw milk production per trimester between 2011 and 2016. A slight seasonal pattern with a peak in Spring (4th trimester) is observable. Over the next 10 years, milk production is projected to grow at a yearly rate between 2.3 and 3.1% yielding an expected production between 42.9 and 47.3 billion litres in 2026 (Ministério da Agricultura, Pecuária e Abastecimento 2016).



Figure 4: Trimestral raw milk production 2011-2016 (Instituto Brasileiro de Geografia e Estatística 2017).

In the case of dairy plants, energy consumption is mainly associated to product quality assurance, especially thermal treatment, refrigeration, and storage (Maganha 2006). In average, approximately 80% of the total energy consumption in a dairy plant is thermal, while the remainder is electric (Maganha 2006). However, energy consumption strongly depends on the type of product, as well as on the adopted processes and the modernity of the used equipment. In average, between 0.14 and 0.33 kWh are consumed per litre of processed milk. A more detailed overview of energy consumption by product type and a list of associated processes and their typical temperatures are shown in Table 2 and Table 3, respectively.

Energy consumption (kWh per litre of product)			
Product	Electricity	Fuel	Total
Milk	0.05	0.12	0.17
Cheese	0.21	1.20	1.41
Butter	0.19	0.98	1.17

Table 2: Type and amount of energy required for dairy goods production (Maganha 2006).

Process	medium	$T$ (°C)
Pasteurization	Water	60-70
Drying (powdered milk)	High-pressure air	120-200
Cleaning	Water	40-50
Sterilization	Water/vapor	60-120
Refrigeration	Air	2-21

Table 3: Typical temperatures of main processes in the dairy sector.

### 2.3. Sugar and ethanol mills

The sugar and alcohol sector is one of the most important ones of the Brazilian economy. According to a survey, 666.8 million tonnes of sugar cane were processed in the 2015-2016

harvest season in the entire country, 92% of which in the Center-South region (União da Indústria da Cana-de-Açúcar 2016).

Sugar cane bagasse thermoelectric plants cover almost 7% of total installed capacity in Brazil (Agência Nacional de Energia Elétrica 2017). An average sugar cane mill processes 2 million tonnes of cane per harvest, during 8 months, usually April-November (Castro, Franco e Mutton 2014). For each ton of processed sugar cane, 260 kg of bagasse are produced. Table 4 shows the energy balance of a typical sugar cane mill. Power and heat for own consumption of a sugar cane mill are usually produced on-site in using sugar cane bagasse.

<b>Operational characteristics</b>	
Harvest period	Apr-Nov (8 months)
Operation hours	5 760 h/y
Processed cane	1 700 000 t
Processed cane per hour	300 t
Energy demand	358 kWh/t <sub>cane</sub>
Vapor demand	180 t/h
Own consumption	9.3 MWh
<b>Bagasse availability</b>	
Bagasse (50%)	467 500 t
Straw	10 000 t
Chips	28 000 t
Total	505 500 t
Relation	2.77 t/MWh
Generated electricity	182 226 MWh
Own consumption	54 400 MWh
Excess production	127 826 MWh

Table 4: Energy balance of typical sugar cane mill.

## 2.4. Integration of STE in agro-industrial applications

Two different integration schemes of solar thermal energy in the agro-industrial systems mentioned above have been considered. The first one applies to consumers currently covering their electricity needs from the grid, while operating an on-site, often biomass-fired, boiler or burner for process heat generation. This case applies to both the abattoir and dairy plant cases. The proposed STE integration scheme foresees the inclusion of a solar/biofuel hybrid central tower receiver plant. Both a Rankine or a Brayton cycle can be considered for the power block, though the higher outlet temperatures of a gas turbine cycle may be preferable if process heat temperatures above 100 °C are envisaged. As net metering policies exist in Brazil, excess solar power is dispatched to the grid.

The second proposed case suits applications in which heat and power are already generated on-site, usually by a biomass-fired Rankine cycle. While heat is typically only used for the consumer's own necessities, excess power is delivered to the grid. This case applies to sugar cane mills. Here, solar-generated heat can be supplied to the power block through a heat exchanger or direct injection of steam, allowing the plant operator to either increase the electricity output of the plant or reduce its biomass consumption.

## 2.5. The SMILE project and the Pirassununga demonstration plant

The SMILE (Solar-Hybrid Micro-Turbine Systems for Co-Generation in Agro-industrial Electricity and Heat Production) Project is carried out by USP in collaboration with DLR and Solinova Ltda. It is financed by the Brazilian National Development Bank, BNDES, under the FUNTEC financing line, Elektro SA under the ANEEL R&D line, and DLR/BMUB. It foresees the construction of two pilot-scale hybrid central tower receiver co-generation plants and their integration with agro-industrial facilities in Pirassununga, São Paulo (21.950° S, 47.453° W) and Caiçara do Rio do Vento, Rio Grande do Norte (5.757° S, 36.002° W), both in Brazil.

In Pirassununga, the plant will be installed on the USP Campus grounds. A 70 kW<sub>el</sub> organic Rankine cycle (ORC) will be employed, delivering 300 kW<sub>th</sub> of process heat at 90 °C. The cycle will be powered by 500 °C air, delivered interchangeably by a 380 kW<sub>th</sub> open volumetric receiver, based on the SolAir concept (Télliez, et al. 2004) or by an auxiliary biodiesel burner. Electricity produced will be delivered to the campus grid, while the heat is going to be supplied to the adjacent abattoir, owned and operated by USP. The project foresees 140 heliostats of 9 m<sup>2</sup> each, to be installed in two phases of 70 units, totalling a reflective area of 1,260 m<sup>2</sup>. Due to the pilot nature of the plant and geometric constraints of the receiver, the expected optical efficiency of the field lies significantly below the optimally achievable value. A process diagram is shown in Figure 5.

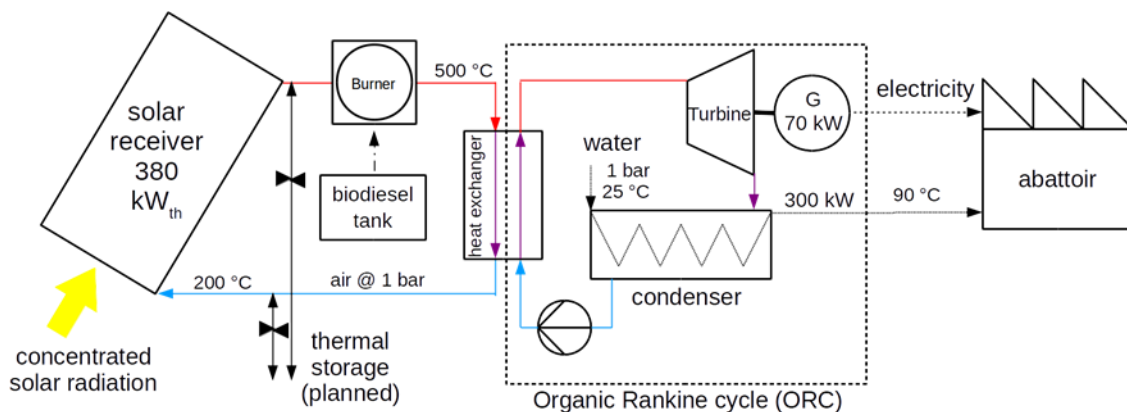


Figure 5: Process schematic of the Pirassununga plant.

In fact, at an earlier project stage, the Pirassununga plant was designed for using a 100 kW<sub>el</sub> micro gas-turbine, powered with 850 °C air heated up in a tubular cavity receiver, based on the SOLHYCO model (Heller 2010). Thanks to the higher efficiency of the gas turbine and lower geometric constraints regarding the receiver, a smaller heliostat field, consisting of 75 heliostats of 8 m<sup>2</sup> each was foreseen. This design had to be scrapped for procurement reasons, but is expected to be more efficient and therefore considered highly promising in the long run. A process diagram for this first setup is shown in Figure 6. In this report, the two plant versions will be addressed as “Pirassununga Setup 1” - the gast turbine plant - and “Pirassununga Setup 2” – the ORC plant.

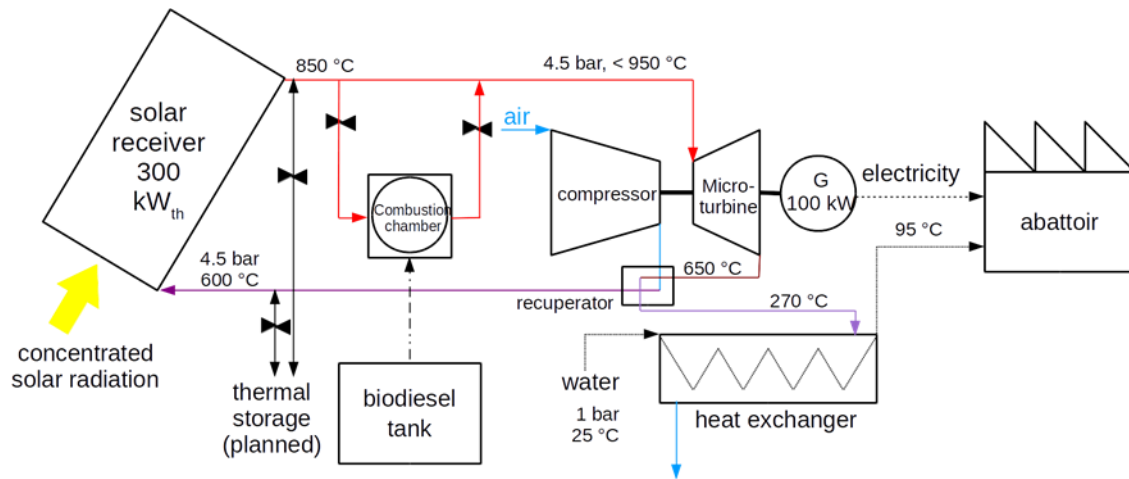


Figure 6: Process schematic of the Pirassununga Setup 1 plant.

The Caiçara plant is owned by the industrial partner Solinova Ltda. Here, the radiation concentrated by 47 heliostats of 9 m<sup>2</sup> each (totally 423 m<sup>2</sup>) will be used to directly generate steam for powering a steam engine. Power and heat generated will be supplied to an adjacent dairy plant. Hybrid operation with bio-diesel is foreseen. Figure 6 shows an artist's view of the Pirassununga Setup 2 and the Caiçara plants.

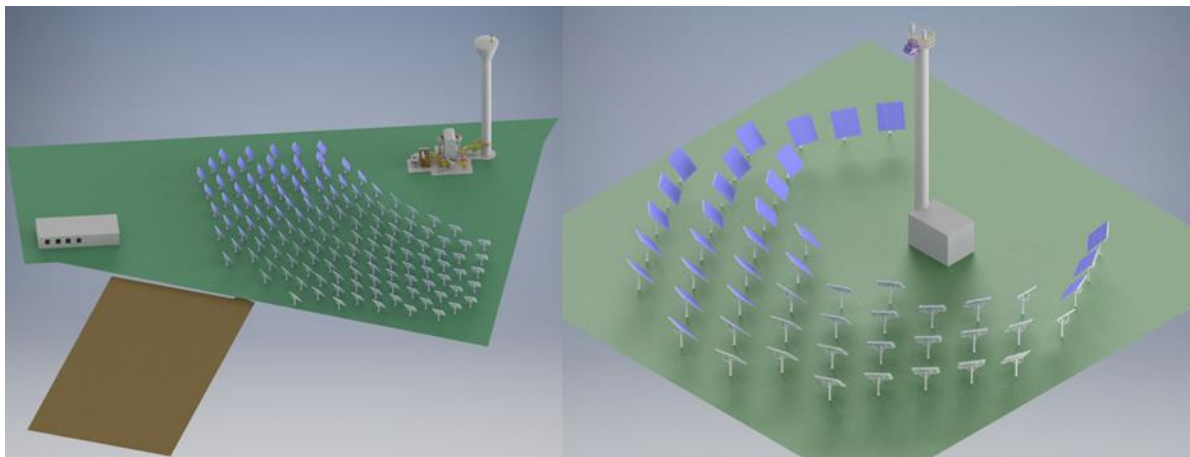


Figure 7: Artist's view of solar/biofuel hybrid plants of the SMILE project in Pirassununga (Setup 2, left) and Caiçara do Rio do Vento (right), Brazil.

In both plants, a novel rim-drive heliostat (Pfahl, et al. 2013) will be employed. Its optical surface of the heliostats consists of nine square facets of 1 m side length arranged in a 3x3 configuration. A deformation approximating a paraboloidal shape is obtained by applying a tension on a central pivot glued to the facet's back side, while the outer parts of the latter rest on a supporting ring. Additionally, the facets are canted with regards to each other. A picture of a mounted prototype at the Pirassununga site is shown in Figure 8. For the Pirassununga Setup 1 plant, a different optical surface, based on bent stripes (Pfahl, Bezerra, et al. 2015), with a total reflective area of 2.5 x 3.2 (W x H) = 8 m<sup>2</sup> was foreseen. The heliostat fields at Pirassununga and Caiçara are currently under installation, thus no experimental data on field performance exist yet. Figure 9 shows the status of the Pirassununga solar field as per January 2018, ready for heliostat installation.



Figure 8: Prototype of the 9 m<sup>2</sup> heliostat being employed in the SMILE project pilot plants.



Figure 9: Installation site for Pirassununga solar plant in January 2018.

### **3. Simulation of central tower receiver systems used in co-generation applications**

The large scale deployment of STE plants in the agro-industrial sector requires the availability of simulation models, able to predict the performance of such plants, to enable fast and cost-efficient pre-dimensioning and feasibility studies. Considering this requirement, two distinct models were developed: model A for a central tower receiver system operating an ORC, based on the Pirassununga Setup 2; model B for a central tower receiver system operating a gas turbine, based on commercially available plants and the Pirassununga Setup 1. Both setups consider the co-generation of electricity and heat, as well as hybridization with biogas

by including a combustion chamber after the solar receiver, enabling a 24/7 of the plant if required.

### **3.1. Tools for simulation of central tower receiver systems**

Two tools were used in the simulation of the STE systems to be integrated in the agro-industry: one for the optical simulation of heliostat field, able to perform the optimization of the heliostat field layout and predict the radiative flux incident on the receiver; another for the simulation of the complete plant, enabling the transient system performance analysis.

For the simulation of the optical components of the plant, Tonatiuh (Blanco, Amieva e Mancillas 2005) was selected. Tonatiuh is an open source Monte Carlo ray-tracing program designed for the analysis and simulation of the optics and energy behaviour of CSP systems. It has several geometric heliostat and receiver shapes and multiple stages can be modelled. Tonatiuh has an inbuilt visualizer, allowing for the generation of flux maps. It is distributed under a GNU general public license which allows free access to the source code for anyone interested in using or contributing to its development. Access to the source code allows a user to develop Tonatiuh to suit almost any application or requirement (Bode e Gauché 2012). Besides a graphic user interface, with a relatively flat learning curve and indicated for simple problems, a scripting interface allows for the solution of more complex and parametrized problems.

For the complete system simulation of the plants, TRNSYS was chosen. TRNSYS was developed at the University of Wisconsin (USA) and has been commercially available since 1975. The software allows the user to model different transient systems using modular components. Each component represents a physical process or resource in the system and these components can be developed and added to the system model according to user's needs. Each component receives input data from a text file and provides an output through the solution of algebraic or differential equations. The components may include solar thermal collectors (parabolic troughs or flat solar collectors, for example), heat exchangers, thermal reservoirs, hydraulic components, among others. Specific processes or sub-components analysis of overall system performance can be modelled (Eustáquio 2011).

There are two key features of TRNSYS: a graphical interface where the system is presented with the components represented by icons and the connections between them represented by lines and the creation of macro components, which are included several components to simplify the visualization of the overall system (Eustáquio 2011).

TRNSYS Simulation Studio platform is one of the most widely used software worldwide for transient simulations, especially of thermal systems. The tool provides predefined templates for components, parameters and input variables that must be set to compose the proper relations between the various components of a simulation. Each component works as a "black box" that receives the input variables and returns the output variables in an iterative rather

than hierarchical solution process, which gives great flexibility to the program (Corgozinho, Neto e Corgozinho 2014).

Other tools which were deemed promising for the tasks at hand, but were ultimately not used, are SAM (Blair, et al. 2014) and SolTrace (Wendelin e Dobos 2013).

### 3.2. Plant model

The next subsections present the main systems' models as well as the plant model developed in TRNSYS for both setups considered for the Pirassununga facility..

#### 3.2.1. Solar Field

For the simulation, all optical imprecisions of the heliostats are subsumed in a surface slope error value, which – due to the absence of experimental data - is assumed to be comparable to that of heliostat models used in commercial systems. Specific assumptions regarding the heliostats considered for the Pirassununga facility are included with the simulation parameters in Table 5.

Optimization of heliostat positions for the fields of the SMILE project was previously carried out by DLR using the STRAL software (Ahlbrink, et al. 2012). Geometric data used in the simulations are shown in Table 5 together with the main simulation parameters used in the Monte Carlo ray-tracing solver of Tonatiuh.

		Pirassununga 1	Pirassununga 2
Heliostat height	m	3.20	3.00
Heliostat width	m	2.50	3.00
Heliostat reflective area	m <sup>2</sup>	8.00	9.00
Mirror reflectance		0.94	0.94
Heliostats focal length	m	30	70
Receiver aperture		circular	rectangular
Receiver area	m <sup>2</sup>	0.64	1.17
Receiver inclination (to vertical)	°	80	20
Center of receiver height	m	25.4	33
Heliostat surface slope error	mrad	3.2	3.2
Slope error distribution		normal	normal
Sunshape		Buie	Buie
Circumsolar ratio		0.02	0.02
Number of rays		10 <sup>8</sup>	10 <sup>8</sup>

Table 5: Heliostat and simulation parameters for the Pirassununga plant, used for the determination of the optical efficiency matrices with Tonatiuh.

The optical efficiency of the field was defined as:

$$\eta_{\text{optical}}(\psi, \theta) = \frac{\dot{Q}_{\text{aperture}}(\psi, \theta)}{A_{\text{field}} DNI}$$

where  $\dot{Q}_{\text{aperture}}$  is the radiative power incident on the receiver aperture,  $A_{\text{field}}$  the total reflective area of the field, and DNI the direct normal irradiance. Using  $30^\circ$  intervals for the azimuth angle  $\psi$  and  $15^\circ$  intervals for the elevation angle  $\theta$  of the sun, an optical efficiency matrix was computed, shown in Figure 10. Nominal values for  $\eta_{\text{optical}}$  (at  $\theta = 90^\circ$ ) are 0.661 for Pirassununga Setup 1, 0.434 for Pirassununga Setup 2, and 0.732 for Caiçara. It has to be noted that the computed values for Pirassununga Setup 2 are relatively low both in comparison to those of commercial fields, as well as to those for Pirassununga Setup 1 and Caiçara. This is due to technical constraints related to the employed receiver, effectively precluding field layouts better suited to the given latitude.

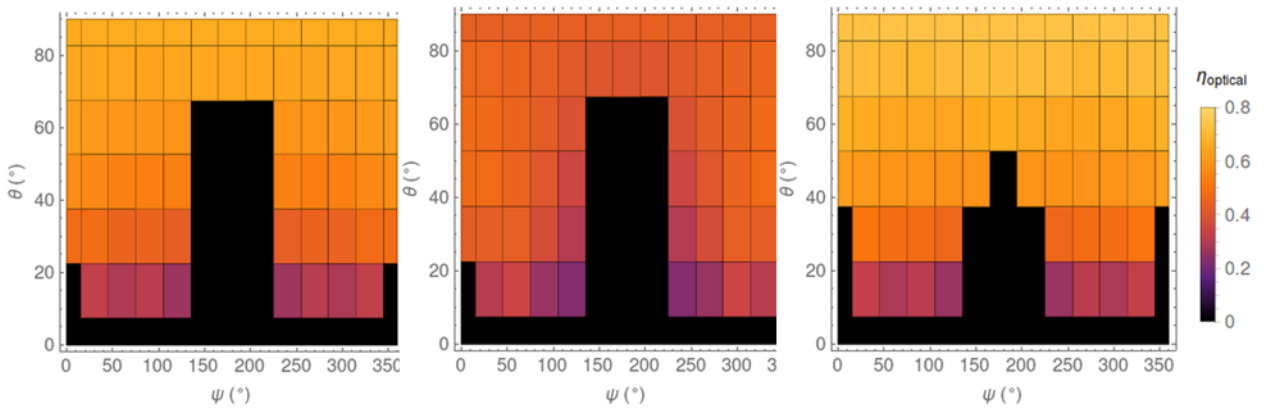


Figure 10: Optical efficiency matrices for Pirassununga Setup 1 (left), Pirassununga Setup 2 (center), and Caiçara (right).

The heliostat field is modelled in TRNSYS by type 394 (Schwarzböl 2006). This type uses information on the solar position at each time step to compute the corresponding solar field efficiency by interpolation of a user supplied efficiency matrix. This information in conjunction with the DNI and the solar field aperture area allows the determination of the solar field radiant power impinging on the receiver according to the following equation:

$$\dot{Q}_{\text{aperture}}(\psi, \theta) = A_{\text{field}} DNI \eta_{\text{optical}}(\psi, \theta) \Gamma$$

where  $\Gamma$  is the fraction of the solar field focusing on the receiver, which is provided by the plant control in order to ensure that the radiative heat flux at the receiver, as well as its temperature, does not exceed the operating conditions. The amount of solar field radiant power lost due to defocusing is given by

$$\dot{Q}_{\text{defocus}}(\psi, \theta) = A_{\text{field}} DNI \eta_{\text{optical}}(\psi, \theta) (1 - \Gamma).$$

### 3.2.2. Receiver model

The receiver is modelled in TRNSYS by type 422 (Schwarzböl 2006). This model was originally developed for pressurized air receivers, however, with some adaptations it can be applied for other types of air receivers due to the flexibility of its physical model. It models the absorber as a grey body to determine the thermal power absorbed by the receiver:

$$\dot{Q}_{\text{absorbed}} = \dot{Q}_{\text{aperture}} \eta_0 - A_{\text{absorber}} \varepsilon \sigma \bar{T}_{\text{absorber}}^4$$

where  $\eta_0$  represents the optical efficiency of the receiver,  $\varepsilon$  the absorber emittance,  $\sigma$  the Stefan-Boltzmann constant,  $A_{\text{absorber}}$  the absorber area and  $\bar{T}_{\text{absorber}}$  the average temperature of the receiver's absorber. Losses at the receiver's piping system can be estimated by

$$\dot{Q}_{\text{loss}} = A_{\text{surf}} [(\varepsilon_s \sigma T_{\text{absorber out}}^4 + h(T_{\text{absorber out}} - T_{\text{env}}))]$$

where  $A_{\text{surf}}$  represents the surface area for the loss computation,  $\varepsilon_s$  the surface's emittance,  $T_{\text{absorber out}}$  the temperature of the air exiting the absorber,  $h$  the surface's convective loss coefficient and  $T_{\text{env}}$  the environment temperature. Other thermal losses can be estimated using a loss coefficient  $f_{\text{loss}}$  such that  $\dot{Q}_{\text{loss}}^{\text{other}} = f_{\text{loss}} \dot{Q}_{\text{absorbed}}$ .

### 3.2.3. Power block model

The power block model depends on the plant design. The Pirassununga Setup 1 plant was designed to use a solarized gas turbine, with a pressurized gas receiver, following a regenerative Brayton cycle. In this case the power block is composed by the air compressor, a regenerator, the turbine, the generator and the combustion chamber. Figure 11 presents a simplified layout for a conventional power block for a gas turbine system. The solar receiver, absent from the figure would be located in the line between the regenerator and the combustion chamber (marked with an x).

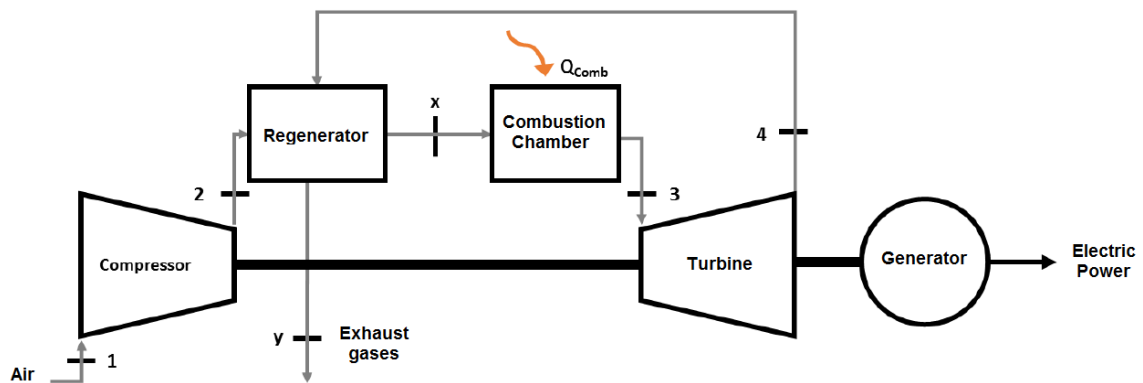


Figure 11: Simplified layout for a gas turbine power block.

The air compressor is modelled by type 424 (Schwarzböl 2006), using the thermodynamic relationships for non-isentropic compression processes. Considering a user supplied isentropic efficiency ( $\eta_{\text{comp, is}}$ ) and the compressor mechanical efficiency ( $\eta_{\text{comp, mech}}$ ), the specific

enthalpy of the outlet air ( $h_{out}$ ) and the work rate ( $\dot{W}_{comp}$ ) required by the compressor is given respectively by

$$h_{out} = h_{in} + \frac{(h_{out,is} - h_{in})}{\eta_{comp,is}} \text{ and}$$

$$\dot{W}_{comp} = \dot{m} \frac{(h_{out,is} - h_{in})}{\eta_{comp,is} \eta_{comp,mech}},$$

were  $h_{in}$  is the specific enthalpy of the air entering the compressor,  $h_{out,is}$  is the outlet air specific enthalpy for the isentropic compression and  $\dot{m}$  the air mass flow rate.

The regenerator is modelled by type 425, a counter-flow gas-gas heat exchanger without capacitance effects, using the inlet mass flow rates, inlet temperatures and the heat exchangers' UA value to compute the heat exchanged and the outlet temperatures.

The gas turbine uses a user defined isentropic efficiency to compute the gas stream outlet conditions and produced work, according to type 427 (Schwarzböhl 2006). Considering the user supplied isentropic efficiency ( $\eta_{turb,is}$ ) and the turbine mechanical efficiency ( $\eta_{turb,mech}$ ), the specific enthalpy of the outlet air ( $h_{out}$ ) and the work rate ( $\dot{W}_{turb}$ ) produced by the turbine is given respectively by

$$h_{out} = h_{in} + \frac{(h_{in} - h_{out,is})}{\eta_{turb,is}} \text{ and}$$

$$\dot{W}_{turb} = \dot{m} \frac{(h_{in} - h_{out,is})}{\eta_{turb,is}} \eta_{turb,mech},$$

were  $h_{in}$  is the specific enthalpy of the air entering the turbine,  $h_{out,is}$  is the outlet air specific enthalpy for the isentropic expansion and  $\dot{m}$  the air mass flow rate.

Finally, the generator was modelled with type 428 which computes the electricity produced according to an user defined efficiency  $\eta_{gen}$  such that  $\dot{P}_{el} = \dot{W}_{turb} \eta_{gen}$ .

The power block for the Pirassununga Setup 2 plant is based on an Organic Rankine Cycle (Figure 12). Public information on the specific operation conditions of its components is not available, thus a simplified black box model for the whole cycle was used, considering available correlations for the electric power produced as a function of the thermal power supplied by the solar system and its auxiliary burner.

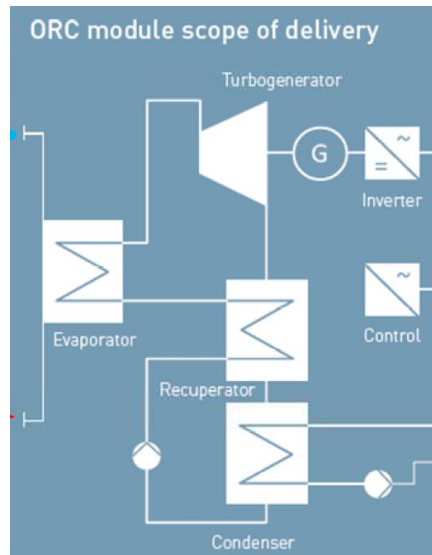


Figure 12: ORC power block.

### 3.2.4. System model

The full system model developed in TRNSYS for the Pirassununga Setup 1 is visible in Figure 13.

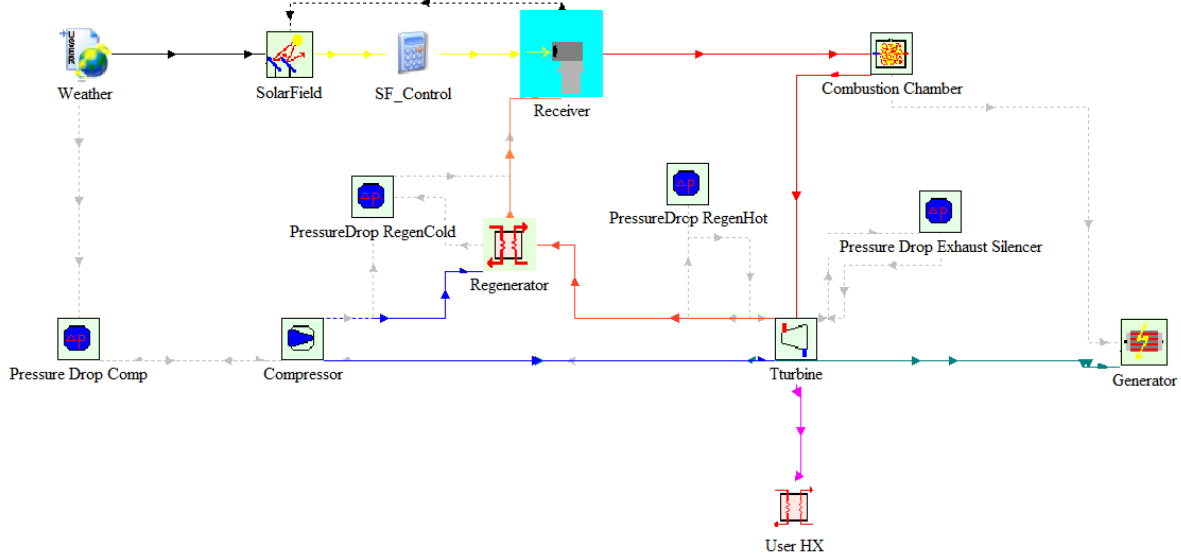


Figure 13:TRNSYS model for the Pirassununga Setup 1 plant.

The system model developed for the Pirassununga Setup 2 is visible in Figure 14. Besides the aforementioned components the system model it is worthwhile mentioning the User Heat Exchanger, a counter-flow air-water heat exchanger enabling the supply of hot water for the Pirassununga abattoir, common to both plant configurations and thus visible in both figures.

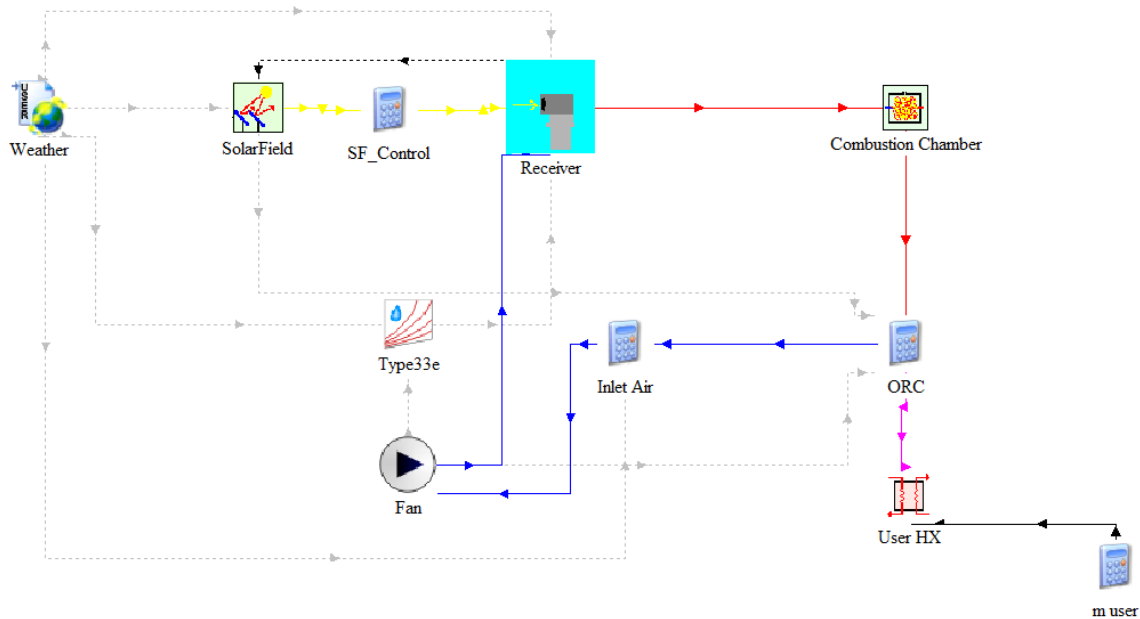


Figure 14: TRNSYS model for the Pirassununga Setup 2 plant.

The design point (DNI = 850 w/m<sup>2</sup>, Sun in zenith) for both plants visible in Table 6.

	Pirassununga 1 (pressurized air receiver)	Pirassununga 2 (open volumetric receiver)
Radiative flux at receiver aperture	532 kW/m <sup>2</sup>	397 kW/m <sup>2</sup>
Solar field power	338 kW	465 kW
Receiver net power	304 kW	412 kW
Receiver efficiency	0.898	0.887
Turbine gross electric power	100 kW	70 kW
Thermal power available for secondary application	170 kW	300 kW

Table 6: Design point for the Pirassununga Setup 1 and 2 plants.

Due to several constrains the Pirassununga pilot plant's commissioning date was postponed to the second half of 2018. Thus, it was impossible to validate the models using experimental data. Instead a verification of the model was performed, comparing the model outputs with the design point information (Table 7).

The Pirassununga 2 model, which corresponds to the pilot plant being actually built, presents results for the receiver net power, turbine gross electric power and thermal power available for heating purposes within 3% of the design values.

	Design value	Simulation result	Relative difference
Receiver net power	412	422.2	2.5%
Turbine gross electric power	70	71.9	2.6%
Available thermal power	300	307.9	2.6%

Table 7: Comparison of the simulation results with the design values for the nominal operating point.

### 3.2.5. Simulation of the Pirassununga facility

Two simulations were performed considering the Pirassununga pilot facility, one for each of the analysed setups. The Pirassununga USP campus abattoir is a teaching facility, thus it presents much smaller energy needs than the commercial facilities due to the reduced workload.

Its main energy requirements are electricity for illumination, equipment operation and cooling, and hot water for cleaning processes. Table 8 summarizes the main energy requirements of this abattoir and the schedule of operation. The energy consumption of this facility has not been monitored, thus two different estimates for the heat requirements are considered, one drawn from the literature (Pacheco e Yamanaka 2006) and another from personal communication with abattoir operators (USP).

<b>Energy requirement</b>				
Total			Literature	USP
	<i>per head</i>	kWh		
	<i>Daily</i>	kWh	605.5	741.2
	<i>Yearly</i>	kWh	221 000	270 546
<b>Electricity</b>				
	<i>percentage</i>		20%	
	<i>per head</i>	kWh		
	<i>Daily</i>	kWh	121	121
	<i>Yearly</i>	kWh	44 200	44 200
... of which for cooling				
	<i>percentage</i>		60%	
	<i>per head</i>	kWh		
	<i>Daily</i>	kWh	73	73
	<i>Yearly</i>	kWh	26 520	26 520
<b>Heat</b>				
	<i>Temperature</i>	°C	< 90	< 90
	<i>per head</i>	kWh		
	<i>Daily</i>	kWh	484	871
	<i>Yearly</i>	kWh	176 800	226 346
<b>Operation period</b>				
Weekdays				
	<i>Factory operation</i>		8-16h	8-16h
	<i>Cooling chamber</i>		0-24h	0-24h
Weekend				
	<i>Factory operation</i>		no	no
	<i>Cooling chamber</i>		0-24h	0-24h

Table 8: Energy consumption of the Pirassununga USP campus abattoir.

Considering the information presented in Table 8, the hourly demand of the facility has been estimated. The electricity demand during weekdays is 3.03 kW between 16h to 8h (which corresponds to the operation of the cooling chamber) and 11.53 for the remainder of the day (corresponding to the operation of the cooling chamber, lighting and equipment). During

weekends the only electrical equipment operating is the cooling chamber, thus an average constant power of 3.03 kW are required.

The facility only has thermal energy demand (hot water) during weekdays between 8h and 16h00, ranging from 85 to 108.8 kW, depending on the chosen information source. It is quite clear from these values that both STE plants considered under the project SMILE are substantially oversized. Since the plant is located in a wider campus with additional facilities the excess electricity will be consumed in other parts of the campus and if any excess energy remains it will be sold to the power grid, considering the possibility to adopt net metering schemes according to Brazilian law. Excess thermal energy will be lost, since no other consumer exists nearby the pilot facility.

### **Pirassununga Setup 2 – Open volumetric receiver with ORC turbine**

During the course of this work the pilot plant configuration was changed due to procurement restrictions. Thus, although a TRNSYS model had already been developed for the Pirassununga Setup 1 plant, the focus of this work was placed onto the study of the Pirassununga Setup 2 plant, a STE plant using an open volumetric receiver operating at 500°C and a ORC turbine.

Simulations have been performed for the Pirassununga Setup 2 plant considering the meteorological data for the year 2016, measured at the plant location. Table 10 summarizes the monthly and annual energy flows in the plant.

Month	Q_solar [MWh]	Q_SF [MWh]	Q_defocused [MWh]	Q_rec [MWh]	Q_fuel [MWh]	Pe_gross [MWh]	Pe_net [MWh]	Q_out_ORC [MWh]	Q_user_high [MWh]	Q_user_USP [MWh]
January	125	48	1	40	261	55	34	236	19	15
February	163	65	2	54	217	50	30	212	18	15
March	165	66	1	55	245	55	34	235	21	17
April	243	95	4	79	210	53	32	227	20	16
May	157	62	2	52	248	55	34	235	19	15
June	180	70	1	58	232	53	32	227	20	16
July	244	94	2	78	221	55	33	235	20	16
August	224	86	4	72	227	55	33	235	20	16
September	215	84	4	70	220	53	32	227	20	16
October	201	77	4	64	235	55	33	235	19	15
November	168	65	2	54	236	53	32	228	20	16
December	194	74	3	62	238	55	33	235	21	17
Annual supply	2278	885	30	737	2790	646	394	2767	236	190

Table 9: monthly and annual energy flows in the Pirassununga Setup 2 plant.

The annual electricity demand of the Pirassununga USP campus' abattoir is estimated to be 44 MWh, while its hot water demand ranges between 192 to 245 MWh per year. According to the performed simulation the system provides 394 MWh of net electricity and between 190 to 236 MWh of thermal energy as hot water. The annual electricity demand is more than covered by the system, while the STE plant supplies between 96 to 99% of the annual thermal energy requirements of the abattoir. It should be mentioned that the available thermal energy for process heating (2767 MWh) is much larger than the demand. However, the hot water is demanded at 90 °C, the temperature of the cooling water exiting from the ORC condenser. If the cooling water is to be circulated in a close circuit, as modelled, then an heat exchanger is

required, and a temperature difference must be established between the ORC condenser's cooling water and the useful hot water exiting the heat exchanger. This is the reason why although larger amounts of thermal energy are available, the STE hybrid plant is not able to fully cover this demand. A different system could be considered, where part of the cooling water exiting the ORC condenser would be directly used by the abattoir. In such situation the system would be able to supply 100% of the electrical and thermal demand of this facility.

It should be also stressed that the considered STE plant is an hybrid plant, equipped with a combustion chamber powered by biogas, ensuring the plant operation at night and during lower irradiance conditions. The relevance of the plant hybridization is also visible in the table, with a significant share of the energy powering the plant coming from the biogas (79%). It is clear from this figure, and as explained before when describing the solar field of this plant that the system is sub-optimal for the location of the plant due to technical constraints related to the employed receiver. This system also presents a high electricity consumption, being 39% of the electricity produced by the plant used in parasitic consumption in the fan, re-cooler, solar field and other systems.

Figure 15 presents the simulated operation temperatures for the STE system under construction in Pirassununga for the weather observed in that location during the 1<sup>st</sup> of February 2016. During the night the combustion chamber powered by biogas maintains the system operating under nominal conditions. As the Sun rises in the morning (around 7:00) the solar field focus solar irradiance onto the receiver, which warms up the incoming air, leading to a decrease in fuel consumption until the solar energy is sufficient for the system operation and the fuel flow is stopped. At this point (around 8:20) the system is fully powered by solar energy. However, with increasing solar energy the receiver temperature rises above 500°C and the plant control starts to defocus part of the heliostats in the solar field, maintaining the receiver operation temperature of 500°C at its outlet. The effects of a disturbance in the solar irradiance are visible between 14:00 and 15:00, requiring the operation of the combustion chamber to ensure the required inlet temperature of 500°C at the ORC inlet.

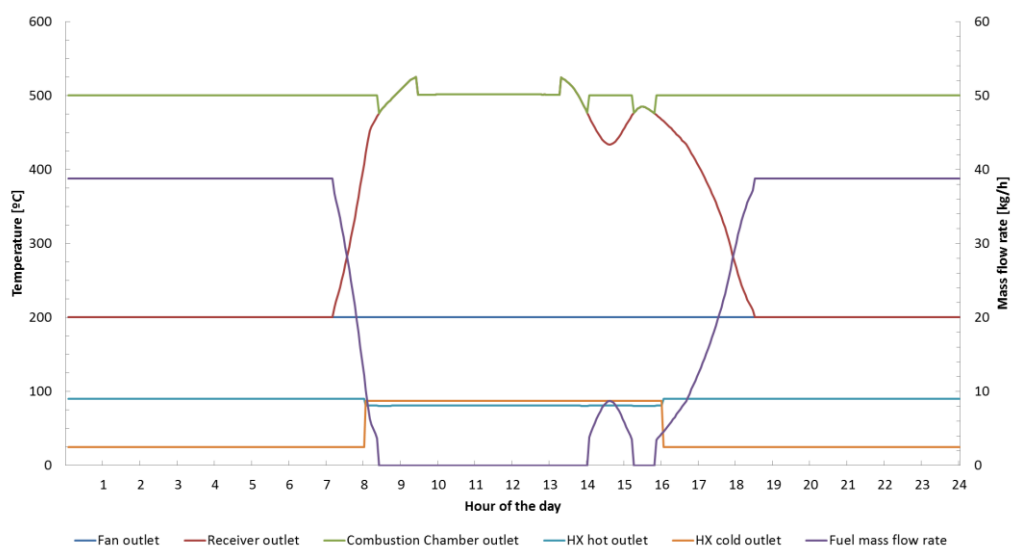


Figure 15: Simulated operation temperatures for the STE system under construction in Pirassununga for a Summer day (1<sup>st</sup> of February 2016).

Also visible in the figure is the operation of the abattoir, translated in the supply of hot water at approximately 90°C between 8:00 and 16:00.

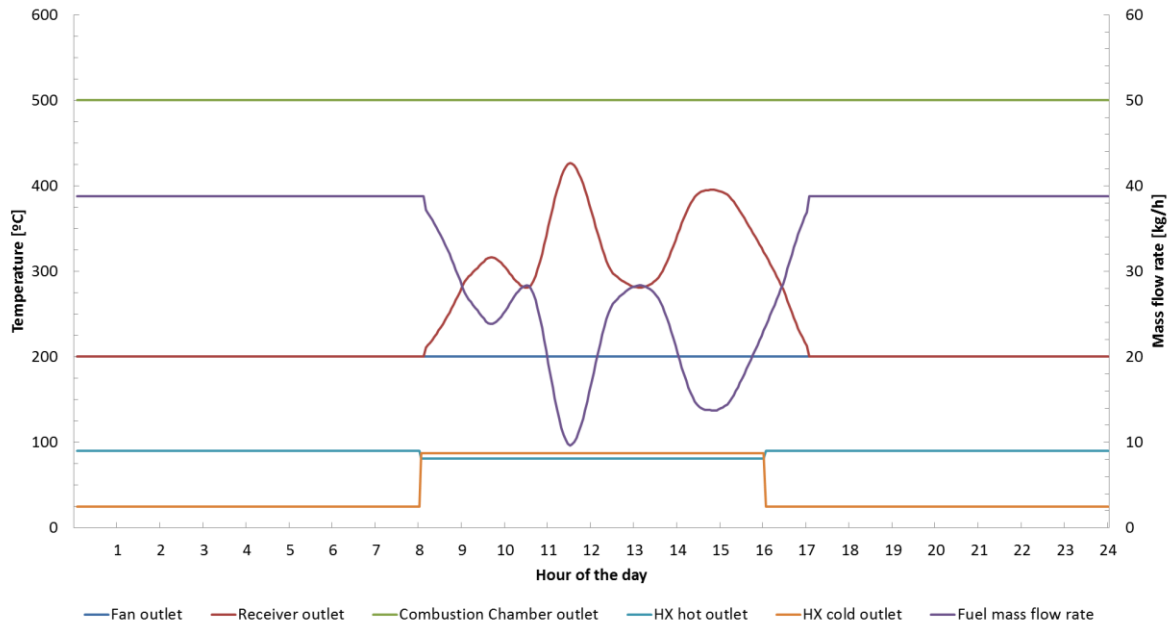


Figure 16: Simulated operation temperatures for the STE system under construction in Pirassununga for a Spring day (11<sup>th</sup> of May 2016).

Figure 16 presents the plant operation for a Spring day with intermittent solar radiance. It is clearly visible the response of the system to the transient behaviour of the available solar radiation. During this day the available DNI is not enough to fully power the system, with the combustion chamber operating throughout the day, albeit at different rates, following the ebbs and flows of the available solar irradiance, visible in the changes of the biogas mass flow rate.

#### 4. Scaling up to industrial plants

Industrial abattoirs in Brazil, namely in the São Paulo state, operate continuously, requiring electricity and heat at all hours of day, throughout all days of the year. Moreover, they operate in a much larger scale than the facility considered in the previous section. The energy consumption for a typical industrial abattoir is presented in Table 10. Three energy requirement levels have been considered, according to the efficiency of the equipment and processes operating in a given facility. Low energy demand facilities require up to 70 kWh of energy per head, while medium energy demand facilities require up to 185 kWh/head and high energy demand facilities consume up to 300 kWh/head of energy (including both electricity and heat) A noticeable difference regarding the USP Pirassununga campus facility, besides the significant increase of energy demand due to the high number of cattle heads processed per day, is the requirement of steam production at temperatures up to 120°C for sterilization purposes and the energy consumption pattern which is constant throughout the day and week in industrial facilities.

Considering the information in the table below, the hourly electricity demand from industrial abattoirs in São Paulo state, Brazil is ranges from 292 kW in low energy requirement facilities

to 1250 kW in high energy requirement facilities. Likewise, the hourly thermal energy demand (steam) ranges from 1167 kW to 5000 kW.

The energy demand of an industrial abattoir is considerably larger than the energy supplied by the STE plants studied in the report. Thus larger STE plants are required to enable a meaningful integration of solar electricity and heat in this agro-industry. However, unless the ORC operating point is changed, increasing the temperature of the water returning from the condenser (used to supply the industrial thermal energy demand), from 90°C to a value above 120°C, a plant based on the Pirassununga Setup 2 will be unable to supply the steam required by an industrial abattoir.

### **Size of consumer**

<b>Heads</b>					
	Daily	/d	500	500	500
	Yearly	/y	182 500	182 500	182 500
<b>Energy requirement</b>			Low	Medium	High
<b>Total</b>					
	<i>per head</i>	kWh	70	185	300
	<i>Daily</i>	kWh	35 000	92 500	150 000
	<i>Yearly</i>	kWh	12 775 000	33 762 500	54 750 000
<b>Electricity</b>					
	<i>percentage</i>		20%	20%	20%
	<i>per head</i>	kWh	14	37	60
	<i>Daily</i>	kWh	7 000	18 500	30 000
	<i>Yearly</i>	kWh	2 555 000	6 752 500	10 950 000
... of which for cooling					
	<i>percentage</i>		60%	60%	60%
	<i>per head</i>	kWh	8	22	36
	<i>Daily</i>	kWh	4 200	11 100	18 000
	<i>Yearly</i>	kWh	1 533 000	4 051 500	6 570 000
<b>Heat</b>					
	<i>Typical temperatures</i>	°C	< 120	< 120	< 120
	<i>per head</i>	kWh	56	148	240
	<i>Daily</i>	kWh	28 000	74 000	120 000
	<i>Yearly</i>	kWh	10 220 000	27 010 000	43 800 000
<b>Operation period</b>					
<b>Weekdays</b>					
	<i>Factory operation</i>		0-24h	0-24h	0-24h
	<i>Cooling chamber</i>		0-24h	0-24h	0-24h
<b>Weekend</b>					
	<i>Factory operation</i>		0-24h	0-24h	0-24h
	<i>Cooling chamber</i>		0-24h	0-24h	0-24h

Table 10: Energy consumption and operation schedule of typical Brazilian abattoirs.

In order to scale up the considered STE plants for integration in industrial abattoirs either a modular approach is considered, installing several small scale plants operating in parallel or a

new plant is designed in accordance with the industrial process demand, presenting a larger solar field, receiver and power block. Taking in consideration both the electrical and thermal nominal power rating for each kind of STE plant analysed in this document it is possible to estimate the required level of scaling up in order to satisfy the power demand from industrial abattoirs.

A facility following the Pirassununga Setup 1 plant (pressurized air receiver with gas turbine) would have to be 3, 8 and 13 times larger, or more powerful, than the pilot plant in order to supply the electric power required by industrial abattoirs with low, medium or large energy requirements. Considering the thermal power requirements such plants would have to be 7, 18 and 29 times larger, or more powerful. Considering a facility following the Pirassununga Setup 2, and assuming the ORC power block could reject heat at temperatures above 120°C to enable its use for the meat industry while maintaining its nominal power rating (which is probably not the case), then such systems would have to be 4, 11 and 18 times larger than the pilot plant in order to supply the electric and thermal power required by industrial abattoirs with low, medium or large energy requirements.

It is then clear that although the pilot facilities being built in Pirassununga are going to be very useful to demonstrate the technology and its potential application to the meat industry, while enabling an experimental learning process about this systems in Brazil, more studies would be required to design facilities suited to the larger energy demand of the industrial abattoirs in Brazil.

## 5. Bibliography

Agência Nacional de Energia Elétrica. *Capacidade de geração do Brasil (Banco de Informações de Geração)*. 2017. <http://www2.aneel.gov.br/aplicacoes/capacidadebrasil/capacidadebrasil.cfm> (último acceso: 4 de October de 2017).

Ahlbrink, Nils, Boris Belhomme, Robert Flesch, Daniel Maldonado Quinto, Amadeus Rong, y Peter Schwarzbözl. «STRAL: Fast Ray Tracing Software With Tool Coupling Capabilities for High-Precision Simulations of Solar Thermal Power Plants.» *Proceedings of the SolarPACES 2012 conference*. Marrakesh, 2012.

Blair, Nate, Aron P. Dobos, Janine Freeman, Ty Neises, y Michael Wagner. *System Advisor Model, SAM 2014.1.14: General Description*. NREL/TP-6A20-61019, Golden: NREL, 2014.

Blanco, Manuel J., Juana Amieva, y Azael Mancillas. «The Tonatiuh Software Development Project: An Open Source Approach to the Simulation of Solar Concentrating Systems.» *ASME 2005 International Mechanical Engineering Congress and Exposition*. Orlando: ASME, 2005. 157-168.

- Bode, S., y P. Gauché. «Review of optical software for use in concentrating solar power systems.» *Proceedings of the South African Solar Energy Conference*. Stekkenbosch, 2012.
- Castro, Sérgio Gustavo Quassi, Henrique Coutinho Junqueira Franco, y Miguel Ângelo Mutton. «Harvest managements and cultural practices in sugarcane.» *Revista Brasileira de Ciência do Solo* 38, nº 1 (2014).
- Corgozinho, I. M., J. H. Martins Neto, y A. A. Corgozinho. «Modelo de simulação de uma planta solar-elétrica utilizando o.» *V Congresso Brasileiro de Energia Solar*. Recife, 2014.
- Eustáquio, J. V. C. S. *Simulação e análise do comportamento do campo de heliostatos de uma central de concentração solar termoelétrica de receptor central*. Master thesis, Porto: Faculdade de Engenharia da Universidade do Porto, 2011.
- Hassine, Ilyes Ben, Mariela Cotrado Sehgelmeble, Robert Söll, y Dirk Pietruschka. «Control Optimization through Simulations of Large Scale Solar Plants for Industrial Heat Applications.» *Energy Procedia* 70 (2015): 595-604.
- Heller, Peter. *SOLHYCO: Solar-Hybrid Power and Cogeneration Plants*. Technical Report 019830, Stuttgart: DLR, 2010.
- Instituto Brasileiro de Geografia e Estatística. *Estatística da Produção Pecuária*. Instituto Brasileiro de Geografia e Estatística, 2017.
- Instituto Brasileiro de Geografia e Estatística. «Levantamento sistemático da produção agrícola (LSPA).» 2017.
- Maganha, M. F. B. *Guia técnico ambiental da indústria de produtos lácteos*. Série P+L, São Paulo: CETESB, 2006.
- Ministério da Agricultura, Pecuária e Abastecimento. *Projeções do Agronegócio: Brasil 2015/2016 a 2025/2026, Projeções de Longo Prazo*. Brasília: Assessoria de Gestão Estratégica, 2016.
- Ministério de Minas e Energia. *Consumo de Energia no Brasil - Análises sectoriais*. Rio de Janeiro: Empresa de Pesquisa Energética - EPE, 2014.
- Organisation for Economic Co-operation and Development. *Improving Energy Efficiency in the Agro-food Chain*. OECD, 2017.
- Pacheco, J. W., y H. T. Yamanaka. *Guia técnico ambiental de abates (bovino e suíno)*. Série P+L, São Paulo: CETESB, 2006.
- Perobelli, Fernando Salgueiro, Admir António Betarelli Junior, Vinicius de Almeida Vale, y Ramon Goulart Cunha. «Impactos Econômicos do Aumento das Exportações Brasileiras de Produtos Agrícolas e Agroindustriais para Diferentes Destinos.» (*Revista de Economia e Sociologia Rural*) 55, nº 2 (2017).

- Pfahl, Andreas, Michael Randt, Carsten Holze, y Stefan Unterschütz. «Autonomous light-weight heliostat with rim drives.» *Solar Energy* 92 (2013): 230-240.
- Pfahl, Andreas, y otros. «Heliostat tailored to Brazil .» *2015 ISES Solar World Congress 2015 Conference Proceedings*. Daegu: ISES, 2015.
- Ramaschiello, Valentina. «Defining agro-industry - A statistical classification perspective.» *FAO-UNIDO Expert Group Meeting on Agro-Industry Measurement*. Rome, 24 - 25 de November de 2015.
- Schwarzböl, Peter. *A TRNSYS Model Library for Solar Thermal Electric Components*. Reference Manual Release 3.0, Köln: DLR and SolarPACES, 2006.
- Silva, Carlos, Doyle Baker, Andrew Shepherd, Chakib Jenane, y Sergio Miranda-da-Cruz, . *Agro-industries for Development*. Rome: The Food and Agriculture Organization of the United Nations and The United Nations Industrial Development Organization, 2009.
- Téllez, Félix, Marianna Romero, Peter Heller, y Ulmer Steffen. «Thermal Performance of “SolAir 3000 kWth” Ceramic Volumetric Solar Receiver.» *12th International Symposium Solar Power and Chemical Energy Systems*. Oaxaca, 2004.
- União da Indústria da Cana-de-Açúcar. «Ranking de produção de cana, açúcar e álcool: região centro-sul e norte-nordeste: safra 2015/2016.» São Paulo: UNião da Indústria da Cana-de-Açúcar, 2016.
- United Nations. «Background Report.» *Global Expert Meeting on Agriculture and Agro-industries Development towards Sustainable and Resilient Food Systems to Inform the 2017 ECOSOC Special Meeting on Innovations for Infrastructure Development and Promoting a Sustainable Industrialization*. 24-26 de April de 2017.
- Wendelin, Tim, y Aron Dobos. *SolTrace: A Ray-Tracing Code for Complex Solar Optical Systems*. NREL/TP-5500-59163, Golden: NREL, 2013.